Macromolecules

Article

pubs.acs.org/Macromolecules

Effect of Ionic Liquid on Structure and Properties of Polysquaraines

Mei-Chan Ho,[†] Ching-Hsun Chao,[‡] Chun-Hua Chen,[†] Ren-Jye Wu,[§] and Wha-Tzong Whang[†,*]

[†]Department of Materials Science and Engineering, National Chiao Tung University, 1001 University Road, Hsinchu, Taiwan, 30010, R.O.C

[‡]Advanced Materials, Electronic Materials, Dow Chemicals, No. 6, Kesi second Road, Jhunan, Miaoli, Science-Based Industrial Park, Taiwan, 35053, R.O.C

[§]Material and Chemical Research Laboratories, Industrial Technology Research Institute, Room 104, Building 67, 195, Sec. 4, Chung Hsing Road, Chutung, Hsinchu, Taiwan, 31040, R.O.C

Supporting Information

ABSTRACT: Polycondensation of 4-bis[2-(1-methylpyrrol-2-yl)vinyl]-2,5-didodecyloxybenzene and squaric acid yielded the polysquaraine **SQ** with two isomeric subunits—1,3-addition (zwitterionic) and 1,2-addition (diketonic) moieties—in the main chain structure. The former featured a C−O/C═O infrared (IR) absorption frequency at 1622 cm^{-1}; the latter, a C═O signal at 1716 cm^{-1}. Traditional synthesis yielded **SQ** as a powder with metallic luster that could not be cast as a polymer film from solution. When the ionic liquid [Oct_3NMe][TfO] (**IL**) was present in the cosolvent of BuOH and benzene (1:3), however, the resulting $\mathbf{SQI}_x$ polymers (x = 0.01−5 wt %) did not precipitate from solution, making it possible to cast continuous free-standing films with a large area (>1 × 1 cm^2). A greater content of **IL** in the solution favored the formation of the 1,3-addition zwitterionic subunits in the $\mathbf{SQI}_x$ polymer main chains, thereby changing the physical and optical properties of the polysquaraine, as evidenced in IR and optical absorption spectra. The features in the UV−Vis−NIR absorption spectra of **SQ** and $\mathbf{SQI}_x$ were dependent on the **IL** concentration and the nature of the solvent. Among our synthesized $\mathbf{SQI}_x$ polymers, $\mathbf{SQI}_{0.01}$ and $\mathbf{SQI}_{0.1}$ formed flexible free-standing films with metallic luster, smooth surfaces, and good semiconductivities (2.27 × 10^{-5} and 4.74 × 10^{-5} S/cm, respectively). X-ray diffraction patterns revealed that the presence of **IL** in the polymerization medium increased the $\mathbf{SQI}_x$ interchain packing distance. $\mathbf{SQI}_{0.01}$ and $\mathbf{SQI}_{0.1}$ possessed thermal stabilities comparable with that of **SQ**. Our successful use of **IL** in the preparation of $\mathbf{SQI}_x$ polymers appears to have great potential for application in ionic liquid−related organic or polymeric preparation and processing.

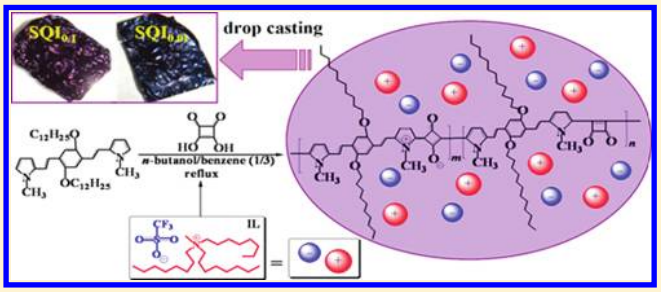

INTRODUCTION

Squaraines, zwitterionic dyes possessing donor/acceptor-type resonance-stabilized structures, exhibit unique optoelectronic properties.[1−3] The combination of intramolecular charge transfer through S_0−S_1 electronic excitation and extended π-conjugated networks gives rise to squaraine dyes displaying intense absorption bands extending from the visible to the near-infrared (NIR) region.[4,5] In general, larger π-conjugated systems and stronger donor/acceptor interactions endow a polymer with a lower optical band gap (E_g)[6] and intrinsic semiconducting properties.[7] Because of their unique optoelectronic properties and intrinsic conductivity, NIR squaraine dyes are used widely in a variety of electronic and photonic materials, with applications in such fields as optical recording,[8,9] solar cells,[10,11] photodynamic therapy,[12,13] laser printing,[14] and infrared (IR) photography.[15]

π-Conjugated squaraine dyes are functional materials with tailorable optoelectronic and photophysical properties, which can be tuned through structural modification to achieve optimal performance. The properties of NIR low-E_g squaraines can be modulated by modifying the π-conjugation length, the nature of the donor/acceptor interactions,[16,17] and the polycondensation reaction conditions. The addition of metal ions in the reaction solution can influence the ratio of the two isomeric repeating units in the polysquaraine[18] and the selectivity and sensitivity of squaraine-based sensors.[19−21] Metal ions also can influence the conformations and photoabsorption spectra of polysquaraines through reversible isomerization.[22,23] Unfortunately, the low solubility of polysquaraines (i.e., intrinsic aggregation) limits their practical applications.[24−26]

Ionic liquids (ILs) are organic salts that usually have melting points below 100 °C. Their melting points are much lower than those of traditional inorganic salts because of the asymmetric structures of the cations and the presence of bulky organic groups, resulting in lower charge density and, in turn, weaker ion pairing interactions.[27,28] In addition, ILs also exhibit low vapor pressures, nonvolatility, good thermal stabilities, high ionic conductivities, and good solubilities in many organic and

Received: November 20, 2011
Revised: February 21, 2012
Published: March 21, 2012

Scheme 1. Polycondensation of Bispyrrole with Squaric Acid in the Presence of IL (Structure Displayed in the Box)

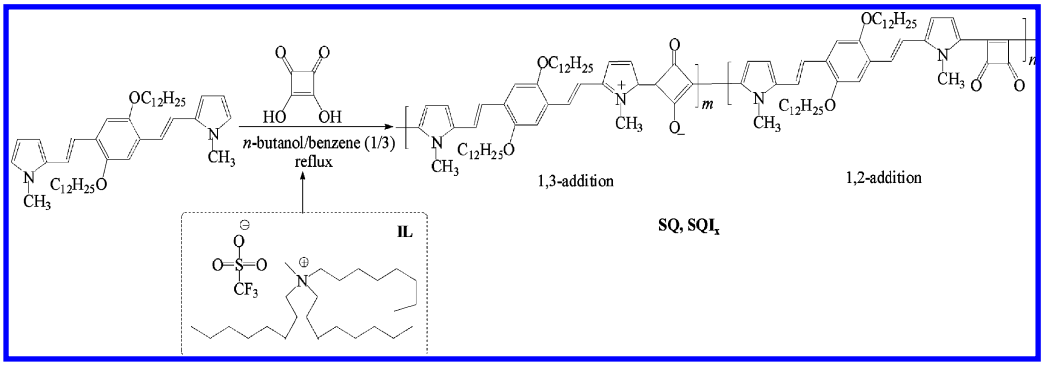

inorganic solvents.[29,30] The solvation and solubility effects of ILs can have favorable effects during chemical and material processing.[31] ILs have also been employed as key components in dispersion media; for example, as solvents in polymerizations,[32] steric stabilizers in organic dispersions,[33,34] and electrolytes for electrochemical polymerizations.[35,36]

For the purposes of easy processing and good free-standing film quality, the methyltrioctylammonium trifluoromethanesulfonate, [Oct_3NMe][TfO] (**IL**), has been used in the preparation of bispyrrole-based polysquaraines (**SQI$_x$**) and in the casting of **SQI$_x$** films. **IL** does not react with either of the monomers during the polymerization leading to **SQ** polymers. Ion−ion solvation interactions between **IL** and the **SQI$_x$** chains can lead to the stable dispersion of **SQI$_x$** polymer chains in solution, thereby decreasing their intrinsic tendency to aggregate and precipitate. Here, we report the influence of **IL** on the structures and physical properties of **SQI$_x$** chains. We used Fourier transform infrared (FTIR) and UV−vis−NIR optical absorption spectrometry to characterize the **SQI$_x$** polymer chains and a four-point probe electrical measurement device, scanning electron microscopy, X-ray diffraction (XRD), and thermogravimetric analysis (TGA) to study their morphological and physical properties.

EXPERIMENTAL SECTION

Materials and Measurements. All reagents were of analytical reagent grade and used as received without further treatment. Hydroquinone (99%, Sigma−Aldrich), 1-bromododecane (98.0%, T.C.I.), K_2CO_3 (anhydrous, 99%, Alfa Aesar), formaldehyde (37% solution, Tedia), AcOH (99.7%, Showa), HBr (33 wt % solution in glacial AcOH, Acros), triethyl phosphite (97%, Sigma−Aldrich), *N*-methylpyrrol-2-carboxaldehyde (98%, Aldrich), squaric acid (99%, Acros), IL (99%, UR-MATOATS), NaH (60% dispersion in mineral oil, Acros), NaCl (99.5%, Showa), $MgSO_4$ (anhydrous, 99%, Showa), MeCN (99.9%, Tedia), MeOH (99.9%, Echo), hexane (99.8%, Echo), $CHCl_3$ (99%, Sigma−Aldrich), tetrahydrofuran (THF, anhydrous, 99.9%, Tedia), CH_2Cl_2 (99.9%, Echo), butanol (99.9%, Echo), and benzene (99.9%, Echo) were obtained from the indicated suppliers. 2,5-Bis(dodecyloxy)-1,4-dibenzyl phosphonate was prepared from 2,5-bis(dodecyloxy)-1,4-bis(bromomethyl)benzene and triethyl phosphite using a previously reported procedure.[37]

Analysis and Characterization. ^1H and ^{13}C NMR spectra were recorded using a Varian Inova (500 MHz) spectrometer and $CDCl_3$ solutions. Fast atom bombardment (FAB) mass spectra were recorded using a MICROMASS TRIO-2000 mass spectrometer. FTIR spectra were measured using KBr pellets on a Perkin−Elmer Spectrum 100 spectrometer. UV−Vis−NIR spectra were recorded using a Jasco V-670 spectrophotometer. The specimens for UV−vis-NIR are prepared by ultrasonically dissolving the formed films following with filtrating (filter paper: pore size =3 μm). The filtrated solution and the corresponding solubility are shown in Figure S5 and Table S1, Supporting Information, respectively. Elemental analyses were performed using a Heraeus CHN-O-RAPID elemental analyzer. TGA curves are performed using a TGA Q500 analyzer, in N_2 atmosphere (99.99%) and operated at a heating rate of 15 °C/min. Powder XRD patterns were performed on a Bruker NanoStar SAXS system (Cu Kα radiation). The electrical conductivities of the polymers were measured using a four-point probe electrical measurement device.

1,4-Bis[2-(1-methylpyrrol-2-yl)vinyl]-2,5-didodecyloxybenzene (Bispyrrole). A N_2-purged flask equipped with a reflux condenser was charged with anhydrous THF (30 mL), NaH (40 mmol), 2,5-bis(dodecyloxy)-1,4-dibenzyl phosphonate (1.8 mmol), and *N*-methylpyrrole-2-carboxaldehyde (3.6 mmol). The mixture was heated under reflux with stirring at 65 °C for 24 h.[38] The dark-yellow solution was concentrated through vacuum distillation; the residue was poured into water and extracted with CH_2Cl_2. The organic layer was dried ($MgSO_4$) and concentrated to give a crude product, which was purified chromatographically (hexane/EtOAc, 25:1) to yield a bright yellow product (76%). ^1H NMR ($CDCl_3$): δ 7.15 (d, J = 16.5 Hz, 2H), 7.05 (d, J = 16.5 Hz, 2H), 6.98 (s, H), 6.63 (s, 2H), 6.49 (m, 2H), 6.15 (t, J = 2.5 Hz, 2H), 4.01 (t, J = 6.5 Hz, 4H), 3.70 (s, 6H), 1.84 (m, 4H), 1.52 (m, 4H), 1.26 (m, 32H), 0.88 (t, J = 7.0 Hz, 6H). ^{13}C NMR ($CDCl_3$): δ 150.95, 132.88, 126.58, 123.44, 121.45, 117.53, 110.94, 108.24, 106.67, 104.99, 69.51, 34.22, 31.92, 29.68, 29.64, 29.50, 29.35, 26.31, 22.69, 14.12. IR (KBr) ν_{max}: 2921, 2847, 1464, 1392, 1284, 1204, 1049, 966, 721 cm^{-1}. FAB-MS m/z: calcd for $C_{44}H_{68}N_2O_2$ [M]$^+$, 656; found, 657.

Poly(bispyrrole-co-squaric acid) (SQ). A solution of **bispyrrole** (0.08 mmol) and squaric acid (0.08 mmol) in butanol and benzene (1:3, 30 mL) was heated under reflux at 120 °C for 24 h and then cooled to room temperature and filtered. The filtrate was concentrated through vacuum distillation and washed sequentially with hexane, Et_2O, and MeOH. The final product was dried in a vacuum oven at 100 °C for 24 h to yield a dark-green powder (70%). IR (KBr) ν_{max}: 2924, 2853, 1716, 1622, 1439, 1347, 1278, 1088, 942 cm^{-1}. Calcd for $(C_{48}H_{66}N_2O_4{\cdot}H_2O)_n$: C, 76.56; H, 9.10; N, 3.72; Found: C, 76.49; H, 8.85; N, 3.99.

Poly(bispyrrole-co-squaric acid) (SQI$_x$). The polymers **SQI$_x$** were prepared in butanol/benzene mixed solvents in which **IL** was present solvent at concentrations (x) in the range 0.01−5 wt %. **Bispyrrole** (0.08 mmol) and squaric acid (0.08 mmol) in butanol and benzene (1:3, 30 mL) were heated under reflux at 120 °C for 24 h. The reaction mixture was cooled to room temperature and filtered to cast thin film (drop casting method). The **SQI$_x$** films were immersed in MeOH to remove any remaining **IL** and then dried in a vacuum oven at 100 °C for 24 h. **SQI$_5$** (5 wt %): powder film; IR (KBr) ν_{max}: 2923, 2852, 1738, 1623, 1439, 1348, 1279, 1092, 944 cm^{-1}. Anal. Calcd for $(C_{48}H_{66}N_2O_4{\cdot}H_2O)_n$: C, 76.56; H, 9.10; N, 3.72. Found: C, 76.48; H, 9.18; N, 3.24. **SQI$_1$** (1 wt %): powder film; IR (KBr) ν_{max}: 2920, 2850, 1736, 1622, 1438, 1347, 1277, 1089, 942 cm^{-1}. **SQI$_{0.1}$** (0.1 wt %): metallic luster film; IR (KBr) ν_{max}: 2920, 2850, 1736, 1620, 1436, 1345, 1272, 1089, 940 cm^{-1}. **SQI$_{0.01}$** (0.01 wt %): metallic luster film; IR (KBr) ν_{max}: 2920, 2850, 1735, 1620, 1436, 1345, 1274, 1088, 940

dx.doi.org/10.1021/ma202526z | *Macromolecules* 2012, 45, 3010−3016

cm^{-1}. Anal. Calcd for $(C_{48}H_{66}N_2O_4{\cdot}H_2O)_n$: C, 76.56; H, 9.10; N, 3.72. Found: C, 74.37; H, 8.79; N, 3.66.

RESULTS AND DISCUSSION

The monomer **bispyrrole** was synthesized and characterized using ^{1}H and ^{13}C NMR spectroscopy, IR spectroscopy, and mass spectrometry. We then polymerized **bispyrrole** with squaric acid to form **SQ** (Scheme 1), a low−band gap polysquaraine that presumably contained 1,2- and 1,3-addition moieties (the latter zwitterionic) in the polymer main chains. The zwitterionic subunits in the **SQ** main chains should have induced strong intermolecular interactions, implying that the polymer would have a strong tendency for aggregation and precipitation from solution. In general, it is hard to find a proper solvent to make quality films of polysquaraines. Thus, we expected **IL** to solvate the zwitterionic polymers well in solution to ensure the absence of precipitation.

Figure 1 reveals the success of our IL-based polymerization approach. The ion−ion interactions between **IL** and **SQ**

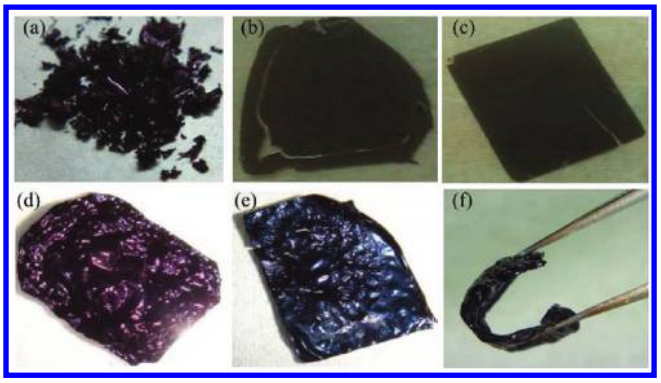

Figure 1. Photographs of (a) the **SQ** powder with metallic luster and (b−e) the **SQI**$_x$ films (b) **SQI**$_5$, (c) **SQI**$_1$, (d) **SQI**$_{0.1}$, (e) **SQI**$_{0.01}$, and (f) flexible **SQI**$_{0.1}$ film.

resulted in the polymer being dispersed stably in solution without precipitation, overcoming the intrinsic aggregation behavior, and finally enhancing the film formation quality. Figure 1a presents a photograph of the broken tiny pieces of the cast SQ film after drying, which had a metallic luster but could not be dissolved in the reaction solvent or any other organic solvent. Figure 1b−e presents photographs of the thin films of **SQI**$_x$ obtained for values of x (**IL** concentration, wt %) of 5, 1, 0.1, and 0.01 respectively. The **SQI**$_5$ and **SQI**$_1$ films were readily crushed, which might originate from the greater conformational relaxation as more **IL** is extracted out, whereas the **SQI**$_{0.1}$ and **SQI**$_{0.01}$ films were of good quality with a large area (>1 × 1 cm^2) and had metallic luster. The free-standing films can be bended without breaking as shown in Figure 1(f). Thus, the properties of these films were affected by the content of **IL**; in other words, a suitable amount of **IL** in the **SQI**$_x$ polymerization solution can optimize the resulting film quality.

FTIR Spectroscopic Structural Analysis. The FTIR spectra in Figure 2 reveal structural information regarding the polymer chains of **SQ** and **SQI**$_x$. At first glance, the features in the FTIR spectra of the polymers **SQ** and **SQI**$_x$ in Figure 2a appear similar. Notably, the characteristic absorptions of **IL** were almost completely absent in the spectra of **SQI**$_x$; that is, **IL** was effectively absent in the final polymeric products. Usually, polysquaraines prepared from **bispyrrole** and squaric acid feature two types of repeating units: 1,3-addition

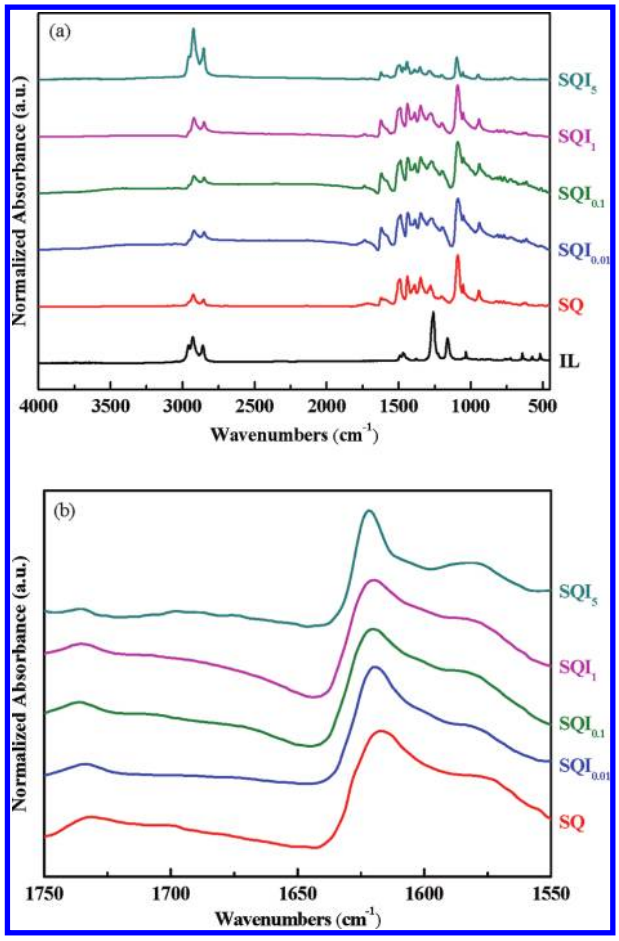

Figure 2. FTIR spectra of neat **IL** and the polysquaraines **SQ** and **SQI**$_x$: (a) 4000−500 cm^{-1}; (b) 1750−1550 cm^{-1}.

(zwitterionic) and 1,2-addition (diketonic) products.[39−42] The FTIR spectroscopic absorptions of the zwitterionic 1,3-addition moieties and weak absorptions at 1716 cm^{-1} for the 1,2-addition (diketonic) moieties. From these FTIR spectra, Table 1 reveals that the 1,3-addition moieties were of the

Table 1. FTIR Spectroscopic Analysis of the Effect of IL on the Main Chain Structures of SQ Powder and SQI$_x$ Films[a]

SQ dye	ν_{C-O} (cm^{-1}) 1,3-addition	intensity	ν_{C-O} (cm^{-1}) 1,2-addition	intensity	ratio 1,3-/1,2-addition
SQ	1622	0.071	1716	0.024	2.96
SQI$_{0.01}$	1619	0.099	1735	0.034	2.91
SQI$_{0.1}$	1620	0.054	1736	0.010	5.40
SQI$_1$	1622	0.232	1736	0.036	6.44
SQI$_5$	1623	0.036	1737	0.005	7.20

[a] **SQI**$_X$:"x" denotes the concentration (wt %) of **IL** relative to the *n*-BuOH/benzene (1:3) reaction solvent.

zwitterionic moieties and weak absorptions at 1716 cm^{-1} for the 1,2-addition (diketonic) moieties. The 1,3-addition moieties were more predominant in **SQI**$_x$ than they were in **SQ**. The ratio of 1,3- to 1,2-addition moieties increased upon increasing the **IL** concentration in the polymerization solution. In other words, the formation of zwitterionic 1,3-addition moieties was more favorable (i.e., they were stabilized) in solutions containing higher **IL** concentrations because of the excellent ion solvation capability of **IL** in polar organic solvents.

dx.doi.org/10.1021/ma202526z | *Macromolecules* 2012, 45, 3010−3016

Since the 1,2-addition moieties have a neutral structure compared with the 1,3-addition ones, the stability is relatively low in the presence of **IL** in the polymerization solution. Therefore, the polycondensation of squaric acid with **bispyrrole** in **IL**-containing solutions favored the production of the 1,3-addition configuration.

Electronic Absorption Spectral Properties. Figure 3 displays the UV−vis−NIR absorption spectra of the poly-

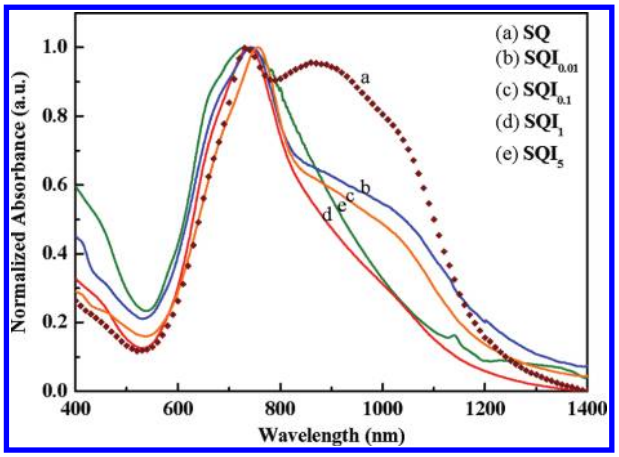

Figure 3. UV−vis−NIR spectra of the polysquaraines **SQ** and $\mathbf{SQI}_x$ in *n*-BuOH/benzene (1:3).

squaraines **SQ** and $\mathbf{SQI}_x$. The spectrum of **SQ** (prepared in the absence of **IL**) featured two intensity maxima at long wavelengths (734 and 874 nm, curve a). $\mathbf{SQ}_{0.01}$ and $\mathbf{SQ}_{0.1}$, which we prepared in the presence of low concentrations of **IL**, featured their maximum intensities at 743−757 nm with a shoulder near 1012 nm (curves b and c, respectively). This feature appears to correlate with the presence of relatively higher ratios of 1,2-addition covalent repeat units. The 1,2-addition structure provides electronic structures of lower symmetry and electronic interactions split into different energy levels, resulting in splitting of the absorption band. Splitting of the absorption bands occurs in the case of mesomeric substituents.[43] Hence, the intensity of the shoulder signal, attributed to the 1,2-addition moieties, decreased upon increasing the ratio of the 1,3-addition moieties. The spectrum of $\mathbf{SQI}_5$, display a maximum absorption at 730 nm, without the shoulder. The absorption peaks at 540−840 nm predominantly represented the electron transitions of the 1,3-addition moieties.

Figure 4 presents the electron absorption spectra of $\mathbf{SQI}_{0.01}$ and $\mathbf{SQI}_5$ prepared in solvents of high (BuOH) and low (benzene) polarity. The spectra of both $\mathbf{SQI}_{0.01}$ and $\mathbf{SQI}_5$ featured broader absorptions when prepared in BuOH than in benzene, with the broadening effect on $\mathbf{SQI}_{0.01}$ being more evident than that on $\mathbf{SQI}_5$. These phenomena are consistent with $\mathbf{SQI}_{0.01}$ featuring a higher ratio of neutral 1,2-diketonic moieties. In the excited state, the 1,2-diketonic structure features significant charge separation,[44,45] with δ^- localized on C═O oxygen atoms and δ^+ accumulated on the pyrrolyl nitrogen atoms, producing a greater change in dipole moment with respect to the ground state than that of the 1,3-moieties, which already possess ionic character. The more highly polar solvent (BuOH) provides greater stabilization of the excited 1,2-moieties, thereby inducing a red−shift of the absorption

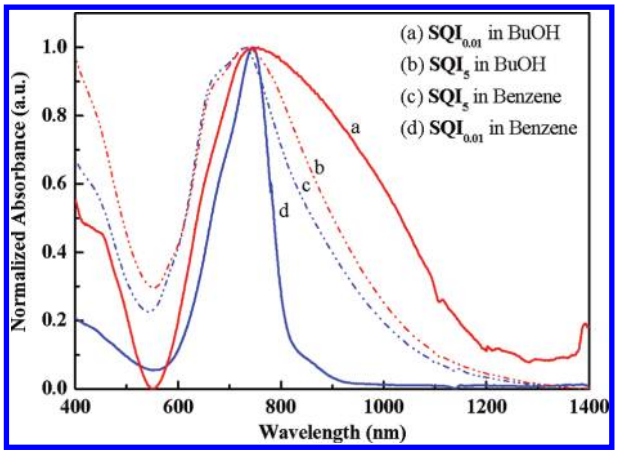

Figure 4. UV−vis−NIR spectra of $\mathbf{SQI}_{0.01}$ (solid line) and $\mathbf{SQI}_5$ (dashed dotted line) in (a, b) *n*-BuOH and (c, d) benzene.

signal. The increase in absorption for $\mathbf{SQI}_{0.01}$ was more evident than that for $\mathbf{SQI}_5$ upon increasing the solvent polarity.

Figure 5 displays the UV−vis−NIR spectra of the polysquaraines $\mathbf{SQI}_{0.01}$ and $\mathbf{SQI}_5$ dissolved in six different solvents. The signals for $\mathbf{SQI}_5$ were relatively unchanged upon increasing the solvent polarity from benzene (lowest polarity) to MeOH (highest polarity). Ionic bonds usually undergo much less of a change in dipole moment upon photon

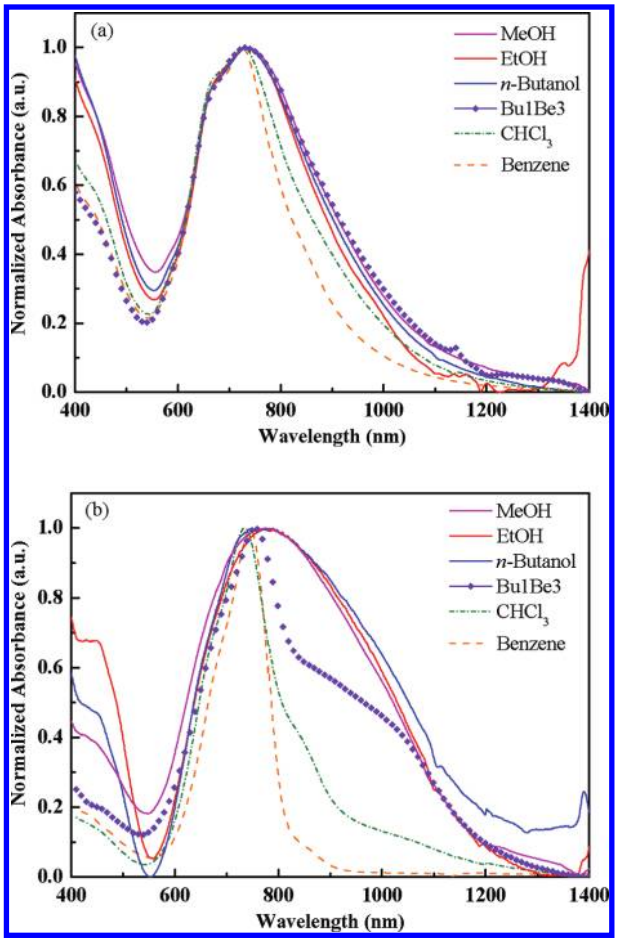

Figure 5. UV−vis−NIR spectra of (a) $\mathbf{SQI}_5$ and (b) $\mathbf{SQI}_{0.01}$ in polar and nonpolar solvents ["Bu1Be3" denotes a mixed solvent of BuOH/benzene (1:3)].

dx.doi.org/10.1021/ma202526z | *Macromolecules* 2012, 45, 3010−3016

absorption than do neutral covalent bonds. Because of its higher content of zwitterionic 1,3-addition moieties, **SQI$_5$** underwent a less significant change in dipole moment upon photon absorption; therefore, the solvent polarity had no significant impact on the photon absorption spectra. In contrast, the spectra of **SQI$_{0.01}$** featured a more noticeable change in absorption upon varying the solvent polarity (Figure 5b). **SQI$_{0.01}$** featured a higher ratio of 1,2-diketone repeat units, which undergo a greater change in dipole moment upon photon absorption. A higher-polarity solvent would better stabilize the dipole moment change upon photon absorption, thereby broadening the absorption spectrum. Hence, the UV–vis–NIR absorption spectrum of **SQI$_{0.01}$** was more sensitive to the solvent polarity.

Surface Morphology and Conductivity. Figure 6 displays the surface morphologies of **SQI$_x$** films prepared

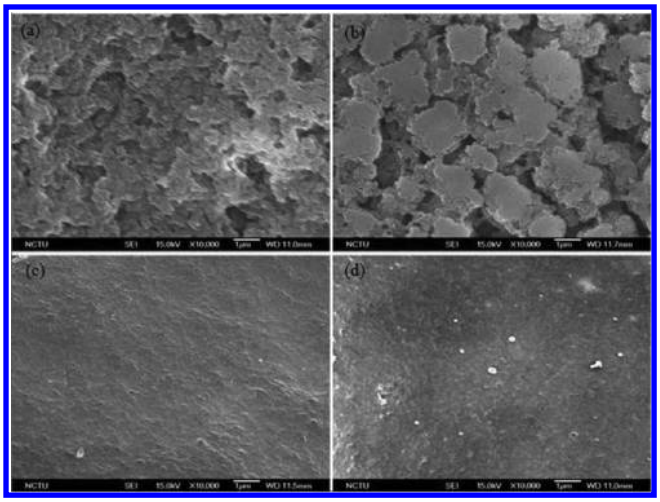

Figure 6. SEM micrographs of the films of (a) **SQI$_5$**, (b) **SQI$_1$**, (c) **SQI$_{0.1}$**, and (d) **SQI$_{0.01}$**.

using the drop casting method. The films of **SQI$_5$** and **SQI$_1$** were readily crushed; their surface morphologies were relatively rough and noncontinuous (Figures 6a and 6b, respectively; cf. Figures 1b and 1c). In contrast, the films of **SQI$_{0.1}$** and **SQI$_{0.01}$** exhibited smooth surfaces, good film quality, and metallic luster (Figure 6, parts c and d; cf. Figure 1, parts d and e). We suspect that this behavior is related to the **IL** content in the drop-casting solution affecting the packing of the polysquaraine chains. A small amount of **IL** in the **SQI$_x$** solution forms a more-stable dispersion of **SQI$_x$**, allowing ready stacking of the chains with less interference from **IL** during the film formation process. In contrast, large amounts of **IL** caused the **SQI$_x$** chains to interact with the; when residual **IL** was removed from the film, the resulting **SQI$_x$** film featured much free space and, therefore, a noncontinuous surface structure.

Table 2 lists the electrical conductivities of the polymers **SQI$_x$**, as measured using the four-point probe method. The conductivities of **SQI$_{0.1}$** and **SQI$_{0.01}$** were 4.74×10^{-5} and 2.27×10^{-5} S/cm, respectively; notably, the former is double the latter. These values are higher than those for **SQI$_1$** and **SQI$_5$**, presumably because of the better molecular close packing and film quality of **SQI$_{0.1}$** and **SQI$_{0.01}$**. Therefore, a low **IL** content in the solution used for polysquaraine preparation enhanced the final polymer film quality, surface morphology, and electrical conductivity.

Table 2. Electrical Conductivities of SQ and SQI$_x$ Films

polymer film	cnductivity (S/cm)
SQ	*a*
SQI$_5$	*b*
SQI$_1$	8.67×10^{-7}
SQI$_{0.1}$	4.74×10^{-5}
SQI$_{0.01}$	2.27×10^{-5}

[a]Powder. [b]not measured.

X-ray Diffraction Studies. The wide-angle X-ray diffraction patterns of solid **SQ** and **SQI$_x$** films (Figure 7) feature

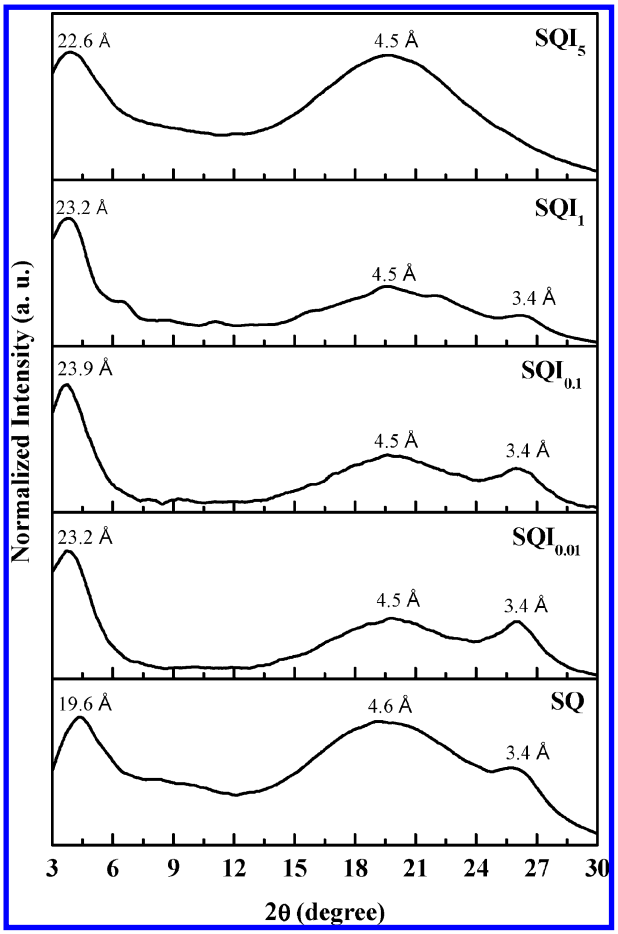

Figure 7. XRD patterns of **SQ** and **SQI$_x$**.

common reflection peaks at angles of 2θ of approximately 4.5 and 3.7–3.9°, corresponding to *d*-spacings of 19.6 and 22.6–23.9 Å, respectively, for the *O*-dodecyl side chains. The interchain packing distance increased from 19.6 Å for **SQ** to 23.9 Å for **SQI$_{0.1}$**, presumably because the presence of **IL** weakened the electrostatic interactions between the **SQ** chains and, thereby, increased the interchain distance. The XRD patterns of the polymers **SQ** and **SQI$_x$** featured broad signals near 19.6–19.2°, corresponding to interlayer spacings of 4.5–4.6 Å. The reflections at values of 2θ near 25.8–26.2° correspond to *d*-spacings of approximately 3.4 Å, consistent with interlayer π-stacking of the **SQ** and **SQI$_x$** chains. The XRD pattern of **SQI$_5$** lacks the signal for π-stacking, presumably because this film possessed a disordered phase associated with more free volume originally occupied by the **IL**. The greater content of **IL** in solution led to more-disordered packing of the

dx.doi.org/10.1021/ma202526z | *Macromolecules* 2012, 45, 3010–3016

polysquaraine layers. Thus, the XRD patterns confirmed the effect of **IL** on the layer packing disorder.

Thermogravimetric Analysis. Figure 8 displays TGA traces of the polymers **SQ** and **SQI**$_x$. These polymers were all

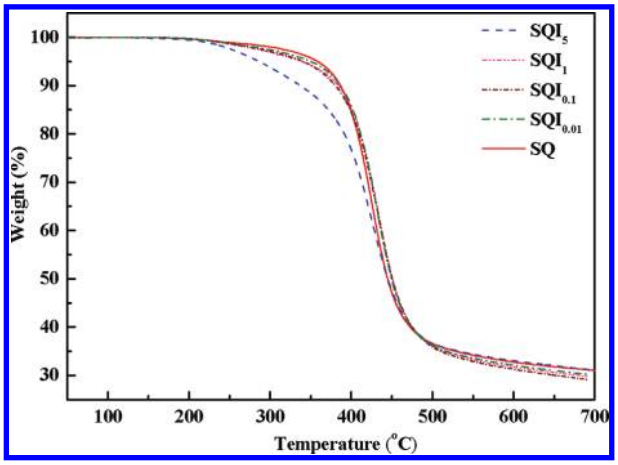

Figure 8. Dynamic thermogravimetric analysis traces of **SQ** and **SQI**$_x$.

very stable at temperatures below 200 °C, exhibiting negligible weight losses. Consistent with a previous report of regarding structural stability, we found that polymer backbones richer in 1,2-addition moieties were more stable than those richer in zwitterionic 1,3-addition moieties.[27] The **SQI**$_x$ polymers featured fewer 1,2-addition moieties than did **SQ**, resulting in their lower thermal degradation temperatures in Figure 8 and Table 3. The dynamic thermal stabilities among the **SQI**$_x$ films

Table 3. Thermal Stabilities of SQ and SQI$_x$ Films

polymer film	T_d[a] (°C)
SQ	357
SQI$_5$	286
SQI$_1$	339
SQI$_{0.1}$	340
SQI$_{0.01}$	349

[a] T_d: Temperature at which 5% weight loss occurred.

followed the trend **SQI$_{0.01}$** > **SQI$_{0.1}$** > **SQI$_1$** > **SQI$_5$**; that is, the greater the content of 1,3-addition moieties on the main chain, the lower the value of T_d. Nevertheless, appropriate control over the **IL** concentration can provide polysquaraines **SQI**$_x$ with thermal stability comparable with that of **SQ**. Therefore, our **SQI**$_x$ polymers that exhibited good film quality has also featured excellent thermally stability, combined with other excellent physical properties.

CONCLUSIONS

The polycondensation of **bispyrrole** with squaric acid results in the formation of polysquaraines featuring both 1,3-addition (zwitterionic) and 1,2-addition (diketonic) moieties. We applied an organic **IL** to the successful preparation of polysquaraine films, because its organic anions and cations solvated the ionic polymer chains effectively in organic solvents. Such solvation induced stable dispersions of the **SQ** chains in solution and decreased the natural tendency for aggregation and precipitation from solution. The polymers **SQI$_{0.01}$** and **SQI$_{0.1}$** provided lustrous semiconductive films exhibiting electron conductivities of 2.27×10^{-5} and 4.74×10^{-5} S/cm, respectively. The presence of **IL** during the polymerization of **bispyrrole** and squaric acid enhanced the ratio of 1,3- to 1,2-addition moieties in the polymers **SQI**$_x$. We attribute this behavior to ion−ion interactions between **IL** and the **SQ** chain's zwitterionic 1,3-moieties, thereby stabilizing the 1,3-addition structures during polymerization. The changing ratio also influenced the UV−vis−NIR absorption spectra and could be used to determine the influence of the solvent polarity on the absorption signals. The UV−Vis absorption spectrum of **SQI$_{0.01}$** was more sensitive to the solvent polarity than was that of **SQI$_5$**. The presence of **IL** in the reaction solutions not only affected the ratio of the two isomeric moieties in the resultant polymers **SQI**$_x$ but also the *d*-spacings for the packing of the *O*-dodecyl side chains. The interchain packing distance increased from 19.6 Å for **SQ** to 23.9 Å for **SQI$_{0.1}$**, due to weaker electrostatic interactions between **IL** and the latter polymer. A suitable concentration of **IL** in the solution enhances the optical properties, film morphology, polymer chain packing, and electrical conductivity, while maintaining excellent thermal stability. We suspect that the use of **IL** as an additive will also have other applications in organic synthesis and polymer chemistry.

ASSOCIATED CONTENT

Supporting Information

The thermal stability of the **IL**, IR absorption spectra of **SQI$_5$** before and after **IL** removing processes, photographs of flexible **SQI$_{0.1}$** film, and the solubility of **SQI$_{0.01}$**. This material is available free of charge via the Internet at http://pubs.acs.org.

AUTHOR INFORMATION

Corresponding Author

*E-mail: wtwhang@mail.nctu.edu.tw.

Notes

The authors declare no competing financial interest.

ACKNOWLEDGMENTS

The authors would like to thank the National Science Council Republic of China, Taiwan, for financially supporting in this research under Grant NSC100-2221-E009-023-MY3.

REFERENCES

(1) Chung, S. J.; Zheng, S.; Odani, T.; Beverina, L.; Fu, J.; Padilha, L. A. *J. Am. Chem. Soc.* **2006**, *128*, 14444−14445.
(2) Shi, Q.; Chen, W. Q.; Xiang, J.; Duan, X. M.; Zhan, X. *Macromolecules* **2011**, *44*, 3759−3765.
(3) Ajayaghosh, A. *Acc. Chem. Res.* **2005**, *38*, 449−459.
(4) Zhang, T. Q.; Tour, J. M. *J. Am. Chem. Soc.* **1998**, *120*, 5355−5362.
(5) Cornelissen-Gude, C.; Rettig, W.; Lapouyade, R. *J. Phys. Chem. A.* **1997**, *101*, 9673−9677.
(6) Ajayaghosh, A.; Eldo, J. *Org. Lett.* **2001**, *3*, 2595−2598.
(7) Zhang, X.; Jenekhe, S. A. *Macromolecules* **2000**, *33*, 2069−2082.
(8) Emmelius, M.; Pawlowski, G.; Vollmann, H. W. *Angew. Chem., Int. Ed. Engl.* **1989**, *28*, 1445−1471.
(9) Natansohn, A. *Macromolecules* **1994**, *27*, 2580−2585.
(10) Silvestri, F. M.; Irwin, D.; Beverina, L.; Facchetti, A.; Pagani, G. A.; Marks, T. J. *J. Am. Chem. Soc.* **2008**, *130*, 17640−17641.
(11) Hagfeldt, A.; Boschloo, G.; Sun, L.; Kloo, L.; Pettersson, H. *Chem. Rev.* **2010**, *110*, 6595−6663.
(12) Cauchon, N.; Tian, H.; Langlois, R.; Madeleine, C. L.; Martin, S.; Ali, H.; Hunting, D.; Lier, J. E. *Bioconjugate Chem.* **2005**, *16*, 80−89.
(13) Comuzzi, C.; Cogoi, S.; Overhand, M.; Van der Marel, G. A.; Overkleeft, H. S.; Xodo, L. E. *J. Med. Chem.* **2006**, *49*, 196−204.

(14) Law, K. Y. *Chem. Rev.* **1993**, *93*, 449−486.
(15) Fabian, J.; Nakazumi, H.; Matsuoka, M. *Chem. Rev.* **1992**, *92*, 1197−1226.
(16) Cho, H. S.; Jeong, D. H.; Cho, S.; Kim, D.; Matsuzaki, Y.; Tanaka, K.; Tsuda, A.; Osuka, A. *J. Am. Chem. Soc.* **2002**, *124*, 14642−14654.
(17) Sreejith, S.; Carol, P.; Chithra, P.; Ajayaghosh, A. J. *Mater. Chem.* **2008**, *18*, 264−274.
(18) Chenthamarakshan, C. R.; Eldo, J.; Ajayaghosh, A. *Macromolecules* **1999**, *32*, 251−257.
(19) Oguz, U.; Akkaya, E. U. *Tetrahedron Lett.* **1998**, *39*, 5857−5860.
(20) Arunkumar, E.; Chithra, P.; Ajayaghosh, A. *J. Am. Chem. Soc.* **2004**, *126*, 6590−6598.
(21) Chenthamarakshan, C. R.; Eldo, J.; Ajayaghosh, A. *Macromolecules* **1999**, *32*, 5846−5851.
(22) Lu, H. C.; Whang, W. T.; Cheng, B. M. *Chem. Phys. Lett.* **2010**, *500*, 267−271.
(23) Lu, H. C.; Whang, W. T.; Cheng, B. M. *J. Mater. Chem.* **2011**, *21*, 2568−2576.
(24) Eldo, J.; Ajayaghosh, A. *Chem. Mater.* **2002**, *14*, 410−418.
(25) Treibs, A.; Jacob, K. *Angew. Chem., Int. Ed. Engl.* **1965**, *4*, 694−695.
(26) Lu, H. C.; Whang, W. T.; Cheng, B. M. *Synth. Met.* **2010**, *160*, 1002−1007.
(27) Seddon, K. R.; Stark, A.; Torres, M. J. *Pure Appl. Chem.* **2000**, *72*, 2275−2287.
(28) Winterton, N. *J. Mater. Chem.* **2006**, *16*, 4281−4293.
(29) Wilkes, J. S.; Levisky, J. A.; Wilson, R. A.; Hussey, C. L. *Inorg. Chem.* **1982**, *21*, 1263−1264.
(30) Welton, T. *Chem. Rev.* **1999**, *99*, 2071−2083.
(31) Lu, J.; Yan, F. *Prog. Polym. Sci.* **2009**, *34*, 431−448.
(32) Kubisa, P. *Prog. Polym. Sci.* **2004**, *29*, 3−12.
(33) Marcilla, R.; Ochoteco, E.; Pozo-Gonzalo, C.; Grande, H.; Pomposo, J. A.; Mecerreyes, D. *Macromol. Rapid Commun.* **2005**, *26*, 1122−1126.
(34) Guerrero-Sanchez, C.; Erdmenger, T.; Sereda, P.; Wouters, D.; Schubert, U. S. *Chem.—Eur. J.* **2006**, *12*, 9036−9045.
(35) Kubo, W.; Kitamura, T.; Hanabusa, K.; Wada, Y.; Yanagida, S. *Chem. Commun.* **2002**, *4*, 374−375.
(36) Ikeda, A.; Sonoda, K.; Ayabe, M.; Tamaru, S.; Nakashima, T.; Kimizuka, N. *Chem. Lett.* **2001**, *11*, 1154−1155.
(37) Arbuzov, B. A. *Pure Appl. Chem.* **1964**, *9*, 307−335.
(38) Eldo, J.; Arunkumarand, E.; Ajayaghosh, A. *Tet. Lett.* **2000**, *41*, 6241−6244.
(39) Lynch, D. E.; Geissler, U.; Peterson, I. R.; Floersheimer, M.; Terbrack, R.; Chi, L. F.; Fuchs, H.; Calos, N. J.; Wood, B.; Kennard, C. H. L.; Langley, G. J. *J. Chem. Soc., Perkin Trans.* **1997**, *2*, 827−832.
(40) Lynch, D. E.; Geissler, U.; Byriel, K. A. *Synth. Met.* **2001**, *124*, 385−391.
(41) Ashwell, G. J.; Jefferies, G.; Green, A.; Skjonnemand, K.; Rees, N. D.; Bahra, G. S.; Brown, C. R. *Thin Solid Films* **1998**, *327*, 461−464.
(42) Chenthamarakshan, C. R.; Eldo, J.; Ajayaghosh, A. *Macromolecules* **1999**, *32*, 251−257.
(43) Lewis, F. D.; Kalgutkar, R. S.; Yang, J. S. *J. Am. Chem. Soc.* **1999**, *121*, 12045−12053.
(44) Neuse, E. W.; Green, B. R.; Holm, R. *Macromolecules* **1975**, *8*, 730−734.
(45) Neuse, E. W.; Green, B. R. *J. Am. Chem. Soc.* **1975**, *97*, 3987−3991.